A model of layer by layer mechanical constraint for additive manufacturing in shape and topology optimization

Grégoire Allaire, Charles Dapogny, Alexis Faure, Georgios Michailidis

12th World Congress on Structural and Multidisciplinary Optimization
5th - 9th, June 2017, Braunschweig, Germany

A model of layer by layer mechanical constraint for additive manufacturing in shape and topology optimization

Grégoire Allaire[1], Charles Dapogny[2], Alexis Faure[3], Georgios Michailidis[4]

[1] CMAP, Ecole polytechnique, CNRS, Université Paris-Saclay, 91128 Palaiseau, France, gregoire.allaire@polytechnique.fr
[2] Laboratoire Jean Kuntzmann, CNRS, Université Grenoble-Alpes, BP 53, 38041 Grenoble Cedex 9, France, charles.dapogny@univ-grenoble-alpes.fr
[3] SIMaP, Université Grenoble-Alpes, BP 53, 38041 Grenoble Cedex 9, France, alexis.faure@simap.grenoble-inp.fr, michailidis@cmap.polytechnique.fr

1. Abstract
We propose a new functional of the domain, to be used in shape and topology optimization problems as a means to enforce the manufacturability of structures by additive manufacturing processes. Instead of considering merely the final shape, it aggregates objective functions (like compliance) for all the intermediate structures of the shape appearing in the course of its layer by layer assembly and subject to their self-weights. We compute its shape derivative and implement it into a shape and topology optimization algorithm based on the level set method. It turns out that this class of constraint functional is very costly to evaluate, due to the large number of successive layers required to build the final shape (each of them requiring a finite element analysis). Therefore, we introduce an interpolation algorithm which significantly accelerates the computational effort. The main idea is to build a piecewise affine approximation of the cost function and of its shape derivative by using the derivative of the elastic displacement with respect to the height of the intermediate structure (this is another application of the concept of shape derivative). Eventually, a numerical validation and some concrete examples are discussed.

2. Keywords: manufacturing constraint, topology optimization, level set method.

3. Introduction
The additive manufacturing technologies have demonstrated a unique potential in realizing structures with a high degree of complexity, thereby allowing to process almost directly the designs predicted by topology optimization algorithms [6]. These breakthroughs however come along with new challenges. One of them is to overcome the difficulty of building shapes showing large *overhangs*, i.e. regions hanging over void without sufficient support from the lower structure. Hitherto, ad hoc criteria, based on a minimum angle between the structural boundary and the horizontal directions, have been used to tackle this issue [5, 7, 8, 9].
In a recent paper [1] we introduced a new geometric and mecanical constraint, related to various processes, including metallic powder bed additive manufacturing, and analysed its mathematical properties. The purpose of the present communication is to give a simple introduction to this model and to show several numerical applications. In metallic powder bed additive manufacturing the structure is built layer by layer. For each layer metallic powder is spread on the bed before it is scanned by the (laser or electron) beam in order to melt the powder in the structural region. At the end of the process, the powder is removed, revealing the final structure Ω. For simplicity, we assume that the components of one single layer of material are built simultaneously during the manufacturing process. In Section 5 we introduce a functional which appraises the constructibility of the shape at each stage of its assembly. In particular, overhang constraints are naturally addressed by this formulation. To achieve our purpose, in the setting of the optimization problem, we distinguish the mechanical situation where the *final* shape Ω is utilized, on which the optimization criterion is based, and that where Ω (and all its *intermediate* structures, see Figure 1) is under construction, which guides the definition of our constraint functional. Our first main result is to provide a shape derivative for this new constraint functional (which is not a standard result because the intermediate upper boundaries are not subject to optimization, being dictated by the additive manufacturing process). It turns out that this class of constraint functional is very costly to evaluate, due to the large number of successive layers required to build the final shape (each of them requiring a finite element analysis). Therefore, we propose a piecewise affine interpolation algorithm, the goal of which is to significantly accelerate the computational effort. The main idea is to build this piecewise affine approximation by using the derivative of the elastic displacement with respect to the height of the intermediate structure (this is another peculiar application of the concept of shape derivative). Eventually, some concrete numerical examples are discussed.

4. Shape optimization problem

A shape is a bounded, regular domain $\Omega \subset \mathbb{R}^d$, $d = 2,3$, filled with a linear elastic material with Hooke's law A. In the context of its final utilization, Ω is clamped on a subset $\Gamma_D \subset \partial\Omega$, and it is submitted to surface loads $f \in L^2(\Gamma_N)^d$ applied on a region Γ_N of $\partial\Omega$ disjoint from Γ_D. The elastic displacement u^m_Ω is the unique solution in $H^1_{\Gamma_D}(\Omega)^d := \left\{u \in H^1(\Omega)^d,\, u = 0 \text{ on } \Gamma_D\right\}$ to the *mechanical* system:

$$\begin{cases} -\mathrm{div}(Ae(u^m_\Omega)) = 0 & \text{in } \Omega, \\ u^m_\Omega = 0 & \text{on } \Gamma_D, \\ Ae(u^m_\Omega)n = 0 & \text{on } \Gamma, \\ Ae(u^m_\Omega)n = f & \text{on } \Gamma_N. \end{cases} \tag{1}$$

For simplicity, the objective $J(\Omega)$ driving the optimization problem is the *compliance*:

$$J(\Omega) = \int_\Omega Ae(u^m_\Omega) : e(u^m_\Omega)\, dx = \int_{\Gamma_N} f \cdot u^m_\Omega\, ds. \tag{2}$$

Our optimization problem then reads:

$$\min_{\Omega \in \mathscr{U}_{ad}} J(\Omega), \text{ such that } P(\Omega) \leq \alpha, \tag{3}$$

in which $\mathscr{U}_{ad}$ is a set of (smooth) admissible shapes Ω, whose boundaries enclose the non optimizable regions Γ_D, Γ_N and Γ_0 (see the next section for its definition), $P(\Omega)$ is a manufacturing constraint, whose definition and properties are discussed in the next sections, and α is a tolerance threshold.

In the context of geometry optimization or of topology optimization by the level set method, the numerical resolution of (3) relies on the shape derivatives of $J(\Omega)$ and $P(\Omega)$, which are defined in the framework of Hadamard's method (see e.g. [3, 10]). A function $F(\Omega)$ of the domain is *shape differentiable* if the underlying mapping $\theta \mapsto F((\mathrm{Id}+\theta)(\Omega))$, from $W^{1,\infty}(\mathbb{R}^d,\mathbb{R}^d)$ into $\mathbb{R}$, is Fréchet differentiable at $\theta = 0$; the corresponding derivative is denoted by $F'(\Omega)(\theta)$. Often, the deformations θ featured in this definition are restrained to a subset $\Theta_{ad} \subset W^{1,\infty}(\mathbb{R}^d,\mathbb{R}^d)$ of admissible displacements, so that deformations $(\mathrm{Id}+\theta)(\Omega)$ of admissible shapes Ω stay admissible. For example, the shape derivative of (2) reads (see e.g. [3])

$$\forall \theta \in \Theta_{ad}, \quad J'(\Omega)(\theta) = -\int_\Gamma Ae(u^m_\Omega) : e(u^m_\Omega)\, \theta \cdot n\, ds.$$

5. Layer by layer mechanical constraint

The constraint $P(\Omega)$ does not apply directly to the *final* shape Ω but rather to the sequence of *intermediate* shapes Ω_h corresponding to different heights h during the additive manufacturing process. More precisely, the shape Ω is enclosed in a cylinder $D = S \times (0,H)$, with cross-section $S \subset \mathbb{R}^{d-1}$, representing the build chamber with a vertical built direction e_d. For any height $h \in (0,H)$, $\Omega_h := \{x = (x_1,...,x_d) \in \Omega,\ 0 < x_d < h\}$ is the intermediate shape describing the stage where Ω is assembled up to height h. The boundary $\partial\Omega_h$ is decomposed in a different fashion from that of $\partial\Omega$ in (1): $\partial\Omega_h = \Gamma_0 \cup \Gamma^l_h \cup \Gamma^u_h$ with

- $\Gamma_0 = \{x \in \partial\Omega_h,\ x_d = 0\}$ is the contact region between Ω and the build table,
- $\Gamma^u_h = \{x \in \partial\Omega_h,\ x_d = h\}$ is the upper side of the intermediate structure,
- $\Gamma^l_h = \partial\Omega_h \setminus \overline{\Gamma_0 \cup \Gamma^u_h}$ is the lateral surface.

Eventually, we define $\ell_h := \{x \in \partial\Omega,\ x_d = h\}$, the part of the boundary $\partial\Omega$ that lies at height h (see Figure 1).

Each intermediate shape Ω_h is clamped on Γ_0, and is only subjected to gravity effects, accounted for by a body force $g \in L^2(\mathbb{R}^d)^d$. Its elastic displacement $u^c_{\Omega_h} \in H^1_{\Gamma^c_D}(\Omega_h)^d$ satisfies:

$$\begin{cases} -\mathrm{div}(Ae(u^c_{\Omega_h})) = g & \text{in } \Omega_h, \\ u^c_{\Omega_h} = 0 & \text{on } \Gamma_0, \\ Ae(u^c_{\Omega_h})n = 0 & \text{on } \Gamma^l_h \cup \Gamma^u_h, \end{cases} \tag{4}$$

The compliance c_{Ω_h} of Ω_h then reads:

$$c_{\Omega_h} = \int_{\Omega_h} Ae(u^c_{\Omega_h}) : e(u^c_{\Omega_h})\, dx = \int_{\Omega_h} g \cdot u^c_{\Omega_h}\, dx. \tag{5}$$

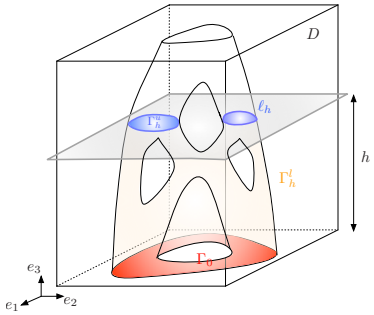

Figure 1: Intermediate shape Ω_h

Our constraint $P(\Omega)$ of the final structure Ω aggregates the compliances of all the intermediate shapes:

$$P(\Omega) = \int_0^H j(c_{\Omega_h})\, dh, \text{ where } j : \mathbb{R} \to \mathbb{R} \text{ is smooth.} \tag{6}$$

It is only incidental that similar mechanical models (that is, linear elasticity systems) are used for describing the mechanical and manufacturing stages. One could very well imagine modelling cooling effects with a constraint involving the temperature of the intermediate shapes Ω_h via the heat equation [2].
Computing the shape derivative of the constraint $P(\Omega)$ is not standard since, when the final shape Ω is varying, only the *lateral* boundaries Γ_h^l of the intermediate shapes Ω_h are allowed to move. This induces some technical difficulties (see [1] for details) and requires a geometric assumption on the shape Ω: we assume that the normal vector $n(x)$ is parallel to the built direction e_d *at most* on a finite number of points $x \in \Gamma_H^l$. In other words, the final lateral boundary Γ_H^l does not contain any 'horizontal flat region'. Under this assumption, and with a specific definition of the set Θ_{ad} of admissible deformation fields θ, we proved in [1] that the shape derivative of $P(\Omega)$, defined by (6), is

$$\forall \theta \in \Theta_{ad}, \quad P'(\Omega)(\theta) = \int_{\Gamma_H^l} \mathscr{D}_\Omega\, \theta \cdot n\, ds, \tag{7}$$

where the integrand factor $\mathscr{D}_\Omega$ is defined for any $x \in \Gamma_H^l$ by:

$$\mathscr{D}_\Omega(x) = \int_{x_d}^H j'(c_{\Omega_h}) \left(2g \cdot u^c_{\Omega_h} - Ae(u^c_{\Omega_h}) : e(u^c_{\Omega_h}) \right)(x)\, dh. \tag{8}$$

The structure of the shape derivative (7)-(8) has an intuitive interpretation: a point x on the lateral boundary Γ_H^l contributes only to the intermediate shapes Ω_h which have height h larger than x_d.
The numerical evaluation of the constraint $P(\Omega)$ and its derivative $P'(\Omega)(\theta)$ rely on a discretization of the height interval $(0,H)$ with a sequence $0 = h_0 < h_1 < \ldots < h_N = H$. The intuitive, 0^{th}-order method to calculate approximations P_N^0 and $\mathscr{D}_N^0$ of $P(\Omega)$ and $\mathscr{D}_\Omega$ consists in replacing c_{Ω_h} and $u^c_{\Omega_h}$ by their respective values at $h = h_{i+1}$ on each interval $I_i := (h_i, h_{i+1})$. Doing so is costly since the subdivision $\{h_i\}_{i=0,\ldots,N}$ of $(0,H)$ has to be fine enough to guarantee the accuracy of this approximation process and at each height h_i one has to solve the elasticity system (4) for the $u^c_{\Omega_{h_i}}$. In [1] we suggested an alternative idea which amounts to compute a 1^{st}-order approximation P_N^1 and $\mathscr{D}_N^1$ of $P(\Omega)$ and $\mathscr{D}_\Omega$. The main idea is to compute the first order derivatives of the mappings $h \mapsto c_{\Omega_h}$ and $h \mapsto u^c_{\Omega_h}$ (which are a special type of shape derivative for the flat upper boundary Γ_h^u). We can then reconsruct on each interval I_i a continuous piecewise affine approximation of $P(\Omega)$ and $\mathscr{D}_\Omega$, which allows us to decrease the number N of intermediate heights.

Figure 2: Optimized design Ω^* for the shape optimization problem (9) without constraint.

6. Numerical examples

Two numerical test cases are presented here. Let us first consider the $2d$ MBB Beam test case: the considered

shapes Ω are contained in a rectangular domain D of size 6×1. Due to symmetry, only half of D is meshed by 300×100 $\mathbb{Q}_1$ elements. In the context of its final utilization (described by the system (1)), the vertical displacement is fixed on a small part of the lower corners, and a unit vertical load $f = (0,-1)$ is applied at the middle of its upper side. When it comes to their construction (modelled by (4)), shapes are built vertically from bottom to top, so that Γ_0 coincides with the lower-side of D.
We first study the simple compliance minimization problem:

$$\min_{\Omega \in \mathscr{U}_{ad}} J(\Omega), \text{ such that } \mathrm{Vol}(\Omega) \leq 0.2\,\mathrm{Vol}(D), \tag{9}$$

where $J(\Omega)$ is the compliance (2). We solve (9), starting from an initial design with many periodically distributed holes, by using an SLP-type algorithm, and the level set method on a fixed Cartesian mesh [3]. The optimized design Ω^* is shown in Figure 2, where several overhanging parts appear.

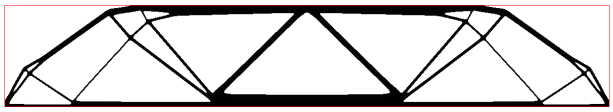

Figure 3: Optimized design Ω^* for the constrained shape optimization problem (10).

We now add our mechanical constraint $P(\Omega)$ to this problem, and now solve:

$$\min_{\Omega \in \mathscr{U}_{ad}} J(\Omega) \text{ such that } \begin{cases} \mathrm{Vol}(\Omega) \leq 0.2\,\mathrm{Vol}(D), \\ P(\Omega) \leq 0.5\,P(\Omega^*). \end{cases} \tag{10}$$

The resulting optimized shape, obtained by using the 0^{th}-order approximation of $P(\Omega)$ and $\mathscr{D}_\Omega$, with a uniform subdivision of $(0,H)$ in $N = 100$ layers, is displayed on Figure 3. The values of the corresponding quantities of interest are collected in Table 1. Notice that several overhangs placed at the lower part of the optimal shape Ω^* without manufacturing constraint have vanished. It is also remarkable that the value of the objective function is lower for the constrained problem, meaning that the constraint has the (surprising) effect of driving the algorithm in a lower local minimum (this may be due to the larger number of iterations in the latter case).

Shape Ω	$J(\Omega)$	$\mathrm{Vol}(\Omega)$	$P(\Omega)$	Iterations	Evaluations
Figure 2	104.165	0.600	0.730	25	38
Figure 3	98.484	0.599	0.343	127	143

Table 1: Values of the shape functionals and iteration numbers for the MBB Beam example

Figure 4: Optimized design Ω^* for the variant (11) of the constrained shape optimization problem (10).

For a better efficiency of our constraint $P(\Omega)$ in order to reduce further overhangs, we propose to replace the elasticity sytem (4) (which has a self-weight gravity force everywhere in the bulk of the shape) by the new system below where only the upper surface is loaded by a constant gravity pressure load

$$\begin{cases} -\mathrm{div}(Ae(u^c_{\Omega_h})) = 0 & \text{in } \Omega_h, \\ u^c_{\Omega_h} = 0 & \text{on } \Gamma_0, \\ Ae(u^c_{\Omega_h})n = 0 & \text{on } \Gamma^l_h, \\ Ae(u^c_{\Omega_h})n = g & \text{on } \Gamma^u_h, \end{cases} \tag{11}$$

and the constraint is still the integral of the compliances over the varying height

$$P(\Omega) = \int_0^H j(c_{\Omega_h})\,dh \quad \text{with} \quad c_{\Omega_h} = \int_{\Gamma^u_h} g \cdot u^c_{\Omega_h}\,ds.$$

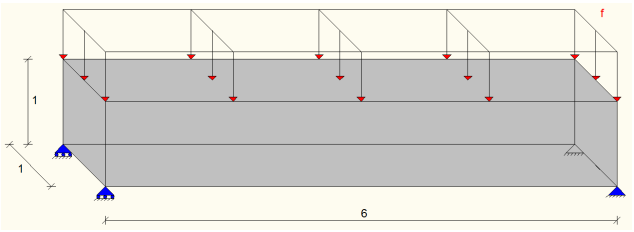

Figure 5: Boundary conditions for the 3d bridge.

This has the effect of penalizing more the horizontal bars in the intermediate shapes and, indeed, it yields designs, as in Figure 4, which have less horizontal bars and the few ones that remain are supported by vertical ones.
Let us consider now a 3d bridge problem with loading conditions given in Figure 5. There is a layer of elements at the top boundary which is not subject to optimization. We first solve (9), without constraint, and the optimized design Ω^* is shown in Figure 6. Since the upper layer is a non-optimizable part, a good strategy is to build this 3d bridge "upside down", that is in the opposite direction $-e_d$. We then solve (10) with our variant (11) of surface

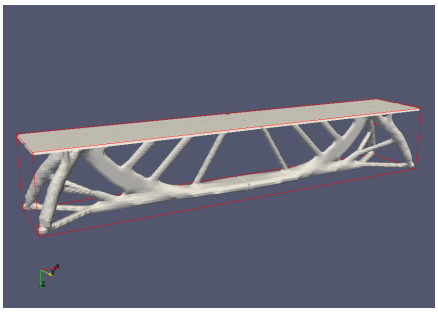

Figure 6: Optimized shape for the 3d bridge without manufacturing constraints.

loadings and with the built direction $-e_d$. The resulting optimized design Ω^* is displayed on Figure 7. One clearly sees that more vertical bars or walls are supporting the lower bar of the bridge.

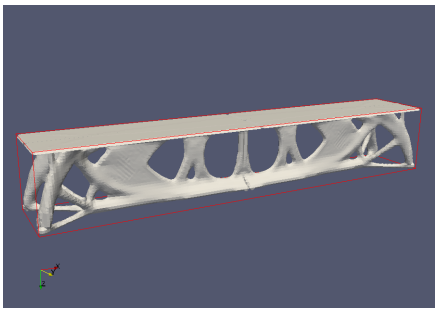

Figure 7: Optimized shape for the 3d bridge with manufacturing constraints.

7. Acknowledgements
This work is partially funded by the DGA and by the SOFIA project. G. A. is a member of the DEFI project at INRIA Saclay Ile-de-France.

8. References

[1] G. Allaire, Ch. Dapogny, A. Faure, G. Michailidis, Shape optimization of a layer by layer mechanical constraint for additive manufacturing, to appear in C. R. Acad. Sci. Paris, Série I. HAL preprint: hal-01398877 (November 2016).

[2] G. Allaire, L. Jakabcin, Taking into account thermal residual stresses in topology optimization of structures built by additive manufacturing, (in preparation).

[3] G. Allaire, F. Jouve and A.M. Toader, Structural optimization using shape sensitivity analysis and a level-set method, *J. Comput. Phys.*, 194, 363-393, 2004.

[4] M.P. Bendsoe and O. Sigmund, *Topology Optimization: Theory, Methods and Applications*, Springer-Verlag, Berlin, 2003.

[5] A.T. Gaynor and J.K. Guest, Topology optimization considering overhang constraints: Eliminating sacrificial support material in additive manufacturing through design, *Struct. Multidisc. Optim.*, (2016), doi:10.1007/s00158-016-1551-x.

[6] I. Gibson, D.W. Rosen and B. Stucker, *Additive manufacturing technology: rapid prototyping to direct digital manufacturing*, Springer Science Business Media, Inc, (2010).

[7] M. Langelaar, Topology optimization of 3D self-supporting structures for additive manufacturing, *Additive Manufacturing*, 12, (2016), pp. 60–70.

[8] A. M. Mirzendehdel and K. Suresh, Support structure constrained topology optimization for additive manufacturing, *Computer-Aided Design*, (2016), http://dx.doi.org/10.1016/j.cad.2016.08.006.

[9] X. Qian, Undercut and overhang angle control in topology optimization: A density gradient based integral approach, *Int. J. Numer. Meth. Engng.*, (2017). DOI: 10.1002/nme.5461.

[10] J. Sokołowski, J.-P. Zolesio, *Introduction to shape optimization: shape sensitivity analysis*, Springer Series in Computational Mathematics, Vol. 10, Springer, Berlin (1992).